Micro Fragmented Adipose Tissue Promotes the Matrix Synthesis Function of Nucleus Pulposus Cells and Regenerates Degenerated Intervertebral Disc in a Pig Model

Xiaopeng Zhou[1,2,]*[iD], Feng Zhang[1,2,]*, Dawei Wang[1,]*, Jingkai Wang[1,2,]*, Chenggui Wang[1,2], Kaishun Xia[1,2], Liwei Ying[1,2], Xianpeng Huang[1,2], Yiqing Tao[1,2], Shouyong Chen[3], Deting Xue[1,2], Jianming Hua[4], Chengzhen Liang[1,2], Qixin Chen[1,2], and Fangcai Li[1,2]

Abstract

Intervertebral disc (IVD) degeneration and consequent lower back pain is a common disease. Micro fragmented adipose tissue (MFAT) is promising for a wide range of applications in regenerative medicine. In this study, MFAT was isolated by a nonenzymatic method and co-cultured with nucleus pulposus cells (NPCs) using an indirect co-culture system *in vitro*. A pig disc degeneration model was used to investigate the regenerative effect of MFAT on degenerated IVDs *in vivo*. The mRNA expression of *Sox9*, *Acan*, and *Col2* in NPCs was significantly increased, while no significant increase was observed in the mRNA expression of proinflammatory cytokine genes after the NPCs were co-cultured with MFAT. Nucleus pulposus (NP)-specific markers were increased in MFAT cells after co-culture with NPCs. After injection of MFAT, the disc height, water content, extracellular matrix, and structure of the degenerated NP were significantly improved. MFAT promoted the matrix synthesis function of NPCs, and NPCs stimulated the NP-like differentiation of MFAT cells. In addition, MFAT also partly regenerated degenerated IVDs in the pig model.

Keywords

intervertebral disc, micro fragmented adipose tissues, nucleus pulposus cell, co-culture, pig disc degeneration model

Introduction

Intervertebral disc (IVD) degeneration and consequent low back pain are major health problems in Western societies and affect 12% to 35% of people in Western countries at some point in their lives, with approximately 10% of individuals becoming disabled[1]. The IVDs lie between the vertebral bodies and act as the joints of the spinal column. The outer annulus fibrosus, the inner nucleus pulposus (NP), and the cartilage endplates form the IVD[2]. A number of large vacuolated cells, named nucleus pulposus cells (NPCs), are located in the NP[3]. The dysfunction of NPCs initiates the loss of extracellular matrix (ECM) and is thought to be the reason for IVD degeneration[4].

Stem cells have great potential to differentiate into various cell types and are usually used as seeding cells in regenerative therapy[5,6]. Mesenchymal stem cells (MSCs) can be used to regenerate degenerated IVDs because they can be

[1] Department of Orthopedics Surgery, the Second Affiliated Hospital, Zhejiang University School of Medicine, Hangzhou, Zhejiang, People's Republic of China
[2] Department of Orthopedics Research Institute of Zhejiang University, Hangzhou, Zhejiang, People's Republic of China
[3] Department of Orthopedics Surgery, The Affiliated Hospital of Hangzhou Normal University, Hangzhou, Zhejiang, People's Republic of China
[4] Department of Radiology, the Second Affiliated Hospital, Zhejiang University School of Medicine, Hangzhou, Zhejiang, People's Republic of China
* These authors contributed equally to this article.

Corresponding Authors:
Fangcai Li, Department of Orthopedics Surgery, the Second Affiliated Hospital, Zhejiang University School of Medicine, 88 Jiefang Road, Hangzhou 310000, Zhejiang, People's Republic of China.
Email: lifangcai@zju.edu.cn

guided to differentiate into an NP-like phenotype under specific environments[7,8]. Growth factors and bioscaffolds are two widely used stimulating factors for inducing MSC differentiation. Our previous studies demonstrated that transforming growth factor-β, insulin-like growth factor (IGF)-1, and fibroblast growth factor (FGF)-2 stimulate the NP-like differentiation of MSCs[9,10]. Other growth factors, such as growth differentiation factors 5 and 6, also been shown to induce the differentiation of MSCs into an NP-like phenotype by other research groups[11,12]. Bioscaffolds incorporated with growth factors and MSCs are often transplanted to regenerate the degenerated NP. ECM-based scaffolds promoted the NP-like differentiation of MSCs *in vitro* and regenerated the degenerated NP in a rat tail disc degeneration model[13]. MSCs cultured in gelatin-based scaffolds also showed increased expression of NP markers[14]. However, MSCs need to be isolated and expanded before transplanting, which may prolong the preparation time of regenerative therapy. In addition, *in vitro* expansion may also alter the biology and decrease the differentiation potential of MSCs[15,16].

MSCs can be derived from bone marrow, adipose tissue, or other tissues[17,18]. Adipose-derived stem cells (ADSCs) are one of the most commonly used MSCs because of their ease of access and high proliferation rate[19]. ADSCs localize in subcutaneous adipose tissues, and traditionally, the stromal vascular fraction (SVF) of subcutaneous adipose tissue is obtained and processed to isolate ADSCs[20]. The SVF of subcutaneous adipose tissue consists of a heterogeneous population of cells, including ADSCs, endothelial precursor cells, pericytes, fibroblasts, and so on[21]. A previous study demonstrated that ADSCs in the SVF play an important role in tissue regeneration and that the SVF can be used as an alternative therapeutic agent in place of ADSCs[22–24]. Directly injecting the SVF decreases the negative effects of pretreatment on the biology and differentiation potential of ADSCs. The SVF has already been used in Achilles tendinopathy treatment, breast reconstruction, and other treatments in clinical trials[25,26]. Comella et al. treated patients with IVD degeneration by intradiscal implantation of SVF plus platelet-rich plasma, and a majority of patients reported improvements in several parameters, including flexion and pain rating[27]. However, the isolation of the SVF by traditional methods such as collagenase does not bode well with regulatory authorities[28]. Adverse effects of the SVF were also observed during the treatment of IVD degeneration in a goat model[29]. Recently, a study reported that micro fragmented adipose tissue (MFAT) that was isolated from adipose tissues using a mechanical method showed better effects in repairing cartilage tissues[30]. The main compositions of the SVF and MFAT are similar, and the most significant difference between the SVF and MFAT is the enzymatic and mechanical techniques used for isolation. Matrix in the MFAT is more similar to adipose tissue compared with that in the SVF. However, the effects of MFAT in regenerating degenerated IVDs are still not clear.

Studies have reported that co-culturing MSCs with NPCs enhances the proliferation and differentiation of MSCs *in vitro*[31]. Moreover, MSCs also increased the expression of matrix gene markers and enhance matrix synthesis in degenerated NPCs in a co-culture system[32]. In addition, MSCs decreased the expression levels of proinflammatory cytokine genes such as IL-1α, IL-1β, IL-6, and TNF-α in degenerative NPCs during co-culture[33]. Both MSCs and NPCs affect each other regarding biology and cell phenotype during co-culture. After transplantation of MFAT into the degenerated IVD, there should also be interactions between NPCs and MFAT. However, the interactions between MFAT and NPCs have not been studied before.

In this study, we aimed to regenerate the degenerated NP directly with MFAT. The co-culture system was used to investigate the interaction effects between MFAT and NPCs, and the inflammatory response of the NPCs to MFAT was also detected during co-culture. We also verified the regenerative effects of MFAT on degenerated IVDs in a pig disc degeneration model. We hope our study will be beneficial for the development of IVD regeneration therapy.

Materials and Methods

Cell Isolation and Culture

Human MFAT were obtained from the liposuction of subcutaneous fat from healthy donors aged from 18–45 years with mild mechanical processes by Lipogems system (Lipogems biotechnology, Shandong, China). The study was approved by the ethics committee of the Second Affiliated Hospital of Zhejiang University School of Medicine. hADSCs were isolated as previously described. Briefly, adipose tissues were washed with phosphate buffered saline and visible blood vessels were removed. Then, tissues were cut into pieces and digested for 40 min at 37°C with 2 mg/mL collagenase type I (Gibco, Shanghai, China). The supernatant was discarded after being centrifuged at 1000 rpm for 5 min. The cell pellet was resuspended with Dulbecco's Modified Eagle Medium (DMEM)-Low Glucose supplemented with 10% fetal bovine serum, 4 mM L-glutamine and 1% penicillin-streptomycin and seeded on a T75 flask. Cells were cultured under static conditions in a humidified incubator at 37°C with 5% CO_2. Medium was completely replaced every 3 days until cells reached confluency. hADSCs at passages 3–5 were then harvested for subsequent experiments. hNPCs were bought from Procell (Procell Life Science & Technology, Hubei, China) and cultured on Matrigel in DMEM-High Glucose supplemented with 10% fetal bovine serum, 4 mM L-glutamine and 1% penicillin-streptomycin solution at 37°C with 5% CO_2. Medium was completely replaced every 3–4 days. hNPCs at passages 3–5 were harvested for subsequent experiments.

Table 1. Primers Used in Quantitative RT-PCR.

Gene	Forward primer (5' to 3')	Reverse primer (5' to 3')
18s	ATCCTCAGTGAGTTCTCCCG	CTTTGCCATCACTGCCATTA
Acan	AGAATCAAGTGGAGCCGTGT	GGTAGTTGGGCAGTGAGACC
Sox9	AGCGAACGCACATCAAGAC	CTGTAGGCGATCTGTTGGGG
Col2	CATCCCACCCTCTCACAGTT	ACCAGTTAGTTTCCTGCCTCTG
Col1	AGTCTGTCCTGCGTCCTCTG	TGTTTGGGTCATTTCCACAT
TNF-α	TCAGAGGGCCTGTACCTCAT	GGAGGTTGACCTTGGTCTGG
IL-1β	CAGAAGTACCTGAGCTCGCC	AGATTCGTAGCTGGATGCCG
IL-6	CTCATTCTGCCCTCGAGCC	TTGTTACATGTTTGTGGAGAAGG
Krt19	GATAGTGAGCGGCAGAATCA	CCTCCAAAGGACAGCAGAAG
Pax1	GACAATCCCAGGCTACCAAG	GCTCCACTCACAAACAGCAA
Gpc3	CCTTTGAAATTGTTGTTCGCCA	CCTGGGTTCATTAGCTGGGTA
Gdf10	ACTTTGACGAGAAGACGATGC	GGTTGGATGGACGAACGAT

Flow Cytometry Analysis and Multi-Lineage Differentiation

hADSCs at passage 3 were used for flow cytometry analysis and to undergo multi-lineage differentiation. MSC surface marker genes (CD34, CD45, CD19, CD90, CD105; eBioscience, Shanghai, China) were detected by a FACS Calibur Cytometer (FACScan, BD Biosciences, San Jose, CA, USA) equipped with CellQuest software (BD Biosciences). For multi-lineage differentiation, hADSCs were cultured for 12 days with osteogenic differentiation medium (Cyagen Biosciences, Guangzhou, China) and stained with alizarin red (Sigma, Shanghai, China). Adipogenic differentiation of hADSCs was performed using an adipogenesis kit (Cyagen Biosciences), and Oil Red O (Sigma) stained after culture for 18 days. hADSCs were cultured for 21 days with chondrogenic differentiation medium[34] and stained with alcian blue (Sigma) to determine the chondrogenic differentiation.

Co-Culture System

Transwell (Corning, Jiangsu, China) and 12-well plates were used as an indirect co-culture system in this study. To study the effects of hNPCs on MFAT and hADSCs, 0.5 mL MFAT or hADSCs were cultured on the plates and hNPCs were seeded into the transwell. The density of hADSCs and hNPCs were both at $1 \times 10^4/cm^2$. To determine the effects of MFAT on hNPCs, hNPCs at a density of $1 \times 10^4/cm^2$ were seeded onto the plates while 0.5 mL MFAT or hADSCs at $1 \times 10^4/cm^2$ were cultured in the transwell. Transwells without cells were set as a control. Cells were cultured in DMEM-High Glucose supplemented with 10% fetal bovine serum, 4 mM L-glutamine and 1% penicillin-streptomycin solution at 37°C with 5% CO_2. The pH level of the culture media was adjusted to pH 6.8 with sterilized HCl (1 M) to represent the mildly degenerated IVD[35,36].

Real-Time Quantitative Polymerase Chain Reaction (RT-PCR)

Cells in the plates were collected and total RNA was extracted with RNAiso reagent (Takara Bio, Beijing, China).

Reverse transcription was performed with PrimeScript™ RT Reagent Kit (Takara Bio) to obtain cDNA, after which the cDNA was diluted with RNAse-free water. The expression levels of mRNA were analyzed utilizing the StepOne-Plus Real-time PCR System (Applied Biosystems, Foster City, CA, USA) and SYBR Green (Takara Bio). The thermal conditions were as follows: 95°C (30 s) for initial denaturation, 40 cycles at 95°C (15 s) and 60°C (30 s). The results were calculated using the $2^{-\Delta\Delta Ct}$ method. All primers were synthesized by Sangon Biotech (Shanghai, China) and 18 s rRNA was used as the housekeeping gene (Table 1).

Western Blot Analysis

Total protein was extracted from the cells cultured in the plates using RIPA Lysis Buffer (Beyotime Biotechnology, Shanghai, China). After being quantified with a BCA protein quantification kit (Beyotime Biotechnology), 30 μg of total proteins were separated with 10% sodium dodecyl sulfate-polyacrylamide gel electrophoresis and transferred to a PVDF transfer membrane (Millipore, Shanghai, China). The membranes were then blocked with 5% skim milk in Tris-buffered saline with 0.1% Tween-20 (TBST) at room temperature for 1 h and hybridized with appropriate primary antibody (SOX9 (1 μg/mL; Abcam, Shanghai, China), aggrecan (1 μg/mL; Abcam), collagen II (0.2 μg/mL; Abcam), collagen I (1 μg/mL; Abcam), KRT19 (1 μg/mL; Abcam), glypican 3 (2.5 μg/mL; Abcam), PAX1 (1.25 μg/mL; Abcam), GDF10 (10 μg/mL; Abcam) or GAPDH (0.1 μg/mL; Santa Cruz, Shanghai, China)) at 4°C overnight. After that, the membranes were incubated with a horseradish peroxidase-labeled secondary antibody (0.1 μg/mL; Santa Cruz) for 1 h at room temperature. The immunoreactive bands were visualized using an enhanced chemiluminescence substrate (Millipore). The expression levels of protein were quantified by densitometry using the Image Lab™ Software (Bio-Rad Laboratories Inc., Munich, Germany).

Animal and Surgical Procedure

All procedures were approved by the Institutional Animal Care and Use Committee of Zhejiang University. Six male BA-MA Mini pigs weighting approximately 25 kg were obtained from the Laboratory Animal Research Center of Zhejiang Chinese Medical University and used for the *in vivo* experiments. Drugs (acepromazine 0.25 mg/kg, ketamine 20 mg/kg, and atropine 0.02–0.05 mg/kg) were injected intramuscularly to pacificate the pigs, and propofol (2 mg/kg) was then injected intravenously to induce full anesthesia. Anesthesia was maintained using 1%–3.5% isoflurane inhaled via the tracheal tube for the duration of the procedure. Autogenous MFAT was obtained from the subcutaneous fat in the groin of pigs by Lipogems system (Lipogems biotechnology). IVD degeneration was induced by the validated pig needle puncture model[37,38]. Each pig's spine was exposed from an anterolateral retroperitoneal approach under sterile conditions. A 16-gauge hollow trochar and cannula was inserted into the NP of L2–L3, L3–L4 and L4–L5 lumber IVDs, and suction was applied to remove 0.5 mL of viscous opalescent fluid. Four weeks after stab, the L2–L3 disc was set as the degeneration group and injected with 200 µL of DMEM, the L3–L4 disc was regarded as the MFAT group and injected with 200 µL of MFAT, and the L4–L5 disc was regarded as the ADSCs group and injected with 200 µL of 2×10^5 autologous ADSCs. The L1–L2 disc was left undisturbed to serve as the control group. After that, the surgical incisions were closed and pigs were permitted free cage activity.

Radiography and Magnetic Resonance Imaging (MRI) Analysis

The lumbar spines of pigs at 0, 4, 8, and 16 weeks after injection were detected by an X-ray system (Philips Digital-Diagnost system, Amsterdam, Netherlands) and a 3.0 T MRI scanner (GE Medical Systems, UK). Pigs were anesthetized and placed in a lateral position before detection. Radiographs were obtained by X-ray system and disc height index (DHI) was calculated[39] and analyzed by two independent and blinded observers. T2-weighted midsagittal sections were obtained by MRI scanner and analyzed. An MRI index (the area of the NP multiplied by the average signal intensity) was used to evaluate the water content and degenerative changes of the NP. The parameter settings of the MRI scanner were as follows: spin echo repetition time, 3200 ms; echo time, 102 ms; field of view, 26×26 cm; slice thickness, 3 mm.

Histological Analysis and Immunohistochemistry

Specimens of from the pigs were harvested at 16 weeks after injection and fixed in 4% paraformaldehyde, decalcified using 10% Ethylene Diamine Tetraacetic Acid, embedded in paraffin, and cross-sectioned (5 µm). Specimens were stained with hematoxylin and eosin (H&E) and safranine O-fast green (S-O), and observed by a microscope (BX51; Olympus, Tokyo, Japan). Immunohistochemical analysis of specimens weas performed as follows: specimens were firstly treated with 3% H_2O_2 for 10 min, and blocked with 5% bull serum albumin for 30 min at room temperature. Then, specimens were hybridized with anti-type II collagen antibody (diluted at 1:200; Abcam, Shanghai, China) at 4°C overnight. Biotin-conjugated second antibody was used to incubate the specimens for 1 h at room temperature. Immunostaining was detected by SABC kit (BOSTER Biological Technology, Wuhan, China) and images were obtained by a microscope.

Biochemical Analysis

NP samples from pigs were obtained at 16 weeks after injection and digested with 125 µg/mL papain (Sigma) for 18 h at 60°C before biochemical analysis. The content of sGAG and hydroxyproline was quantified by Blyscan assay (Biocolor, Beijing, China) and Hydroxyproline Assay Kit (Jiancheng Bioengineering Institute, Jiangsu, China) following the manufacturer's protocol and normalized with sample dry weight.

Statistical Analysis

Statistical analysis was performed with SPSS software package (Version 22.0 for Windows, SPSS Inc., USA). All experiments were performed in triplicate at minimum, and data were assessed for normality using the Shapiro Wilks Normality test. The data passing normality were presented as mean $\pm$ standard error of mean. The statistical significance of the differences between experimental groups was determined with a two-tailed Student's *t*-test or one-way analysis of variance (ANOVA) following Tukey's post hoc test. A value of $p < 0.05$ was considered statistically significant.

Results

Isolation and Characterization of hADSCs

hADSCs at passage 3 were characterized by the detection of surface markers and multi-lineage differentiation ability. hADSCs had high expression of mesenchymal surface markers, including CD90 and CD105, and lacked expression of the primitive hematopoietic progenitor and endothelial cell marker CD34, the pan-leukocyte marker CD45, and the B cell marker CD19 (Fig. 1A). Alizarin red staining was positive after 12 days of culture in osteogenic medium, and the mineral deposition was stained red. hADSCs were induced by adipogenic differentiation medium for 18 days and stained with Oil Red O. Positive staining was observed after cells were cultured in chondrogenic differentiation medium for 21 days and stained with alcian blue (Fig. 1B).
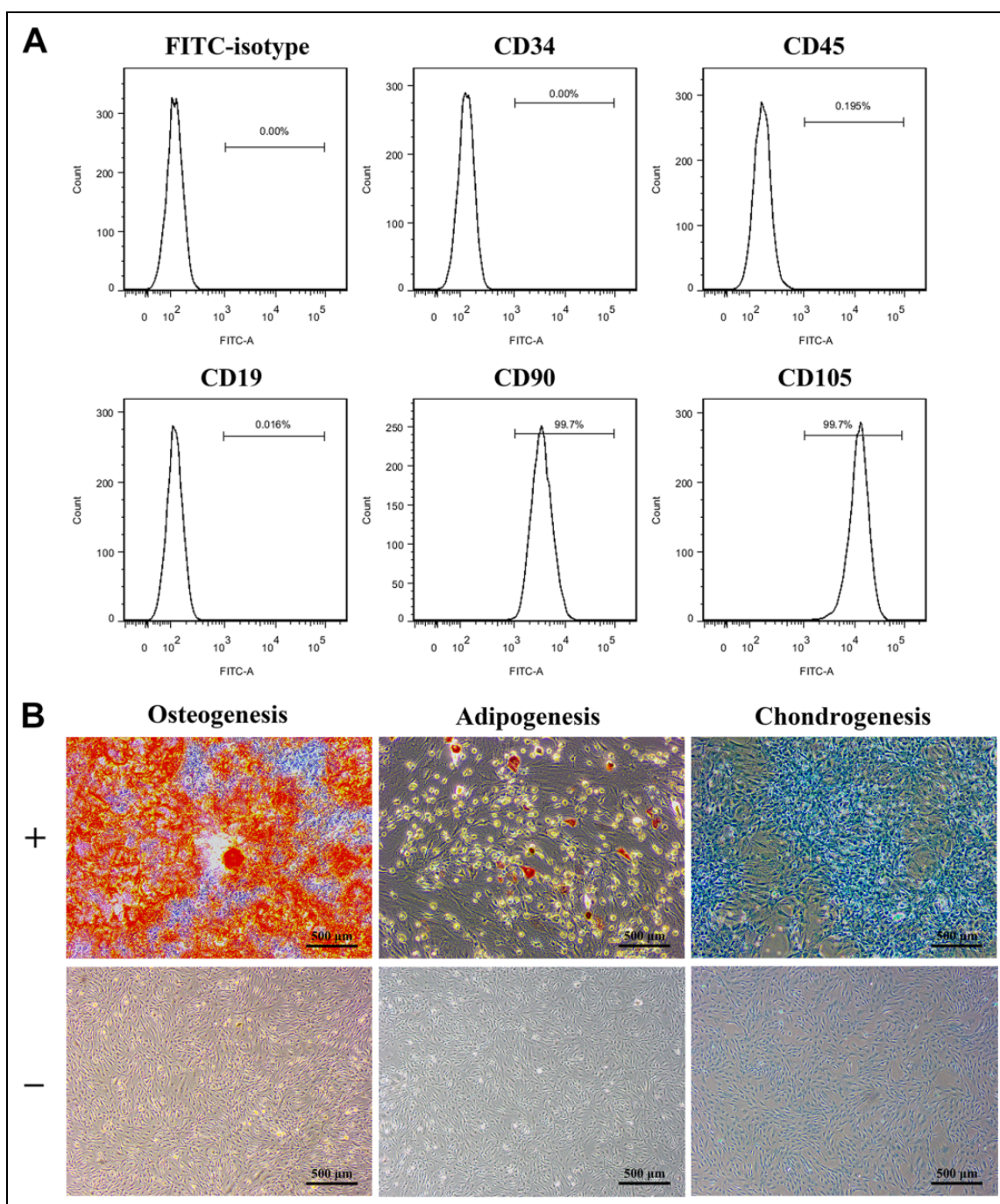
Figure 1. Isolation and characterization of hADSCs. (A) Cell surface markers expressed by hADSCs were determined by flow cytometry. (B) The multi-lineage differentiation of hADSCs were confirmed by alizarin red staining, Oil Red O staining, and alcian blue staining. hADSCs cultured on plates without induction of differentiation was set as control. $N=9$; Scale bar $= 500$ μm.

Effects of MFAT and hADSCs on the Matrix Synthesis Function of hNPCs

After co-culture with hADSCs, the gene expression of *Acan*, *Sox9*, *Col2*, and *Col1* in hNPCs did not change significantly on days 7 and 14 ($p > 0.05$). However, the gene expression of *Acan*, *Sox9*, and *Col2* increased significantly in the MFAT

group compared with those of the other two groups on both days 7 and 14 ($p < 0.01$). No significant difference was observed among the three groups in the gene expression of *Col1* on day 7 or 14 ($p > 0.05$, Fig. 2A). We also measured the protein expression levels of aggrecan, SOX9, COL2, and COL1 on day 21 to show the matrix synthesis function of hNPCs. The MFAT group had the highest expression levels
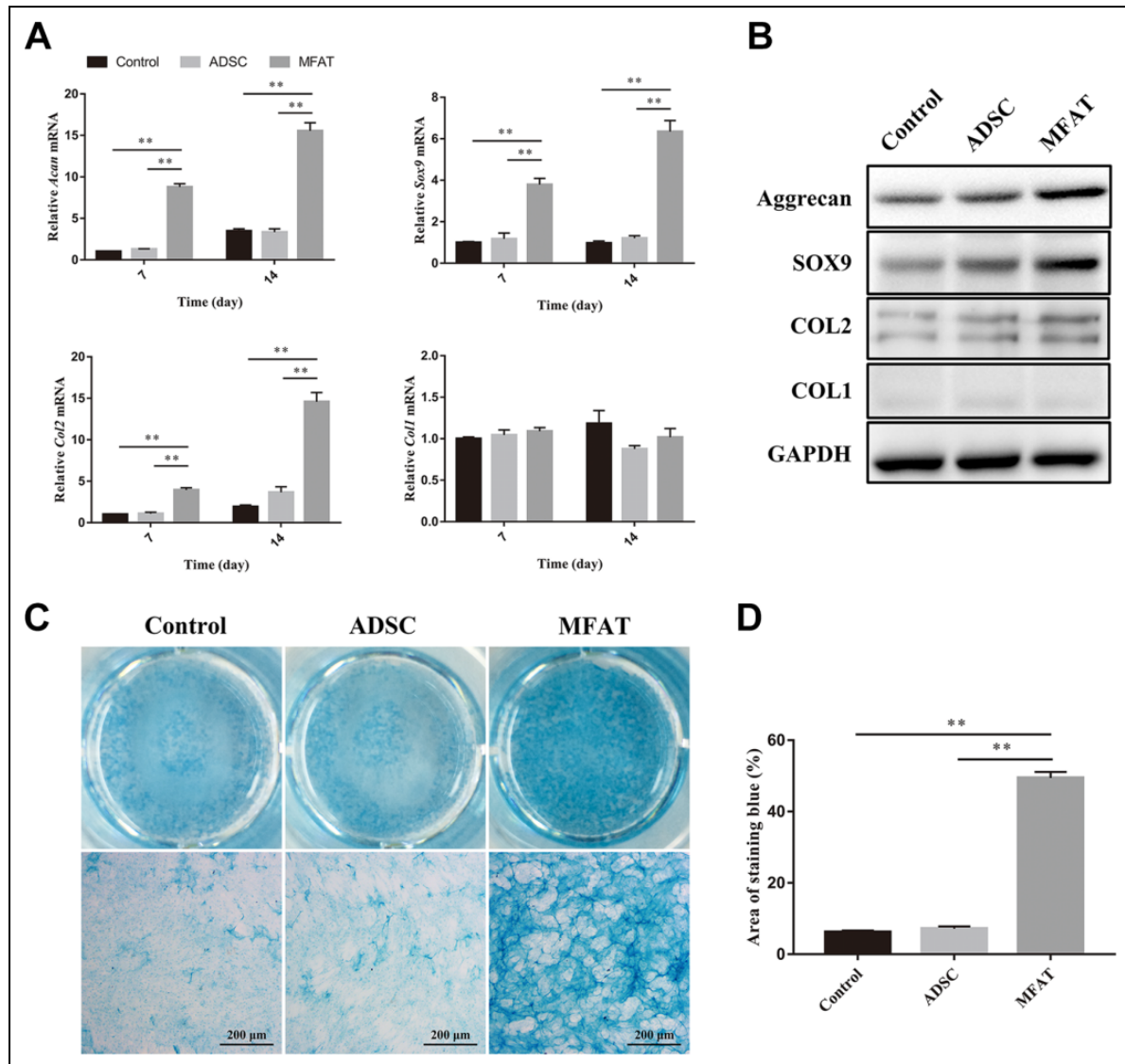
Figure 2. Effects of MFAT and hADSCs on the matrix synthesis function of hNPCs. (A) Gene expressions of Acan, Sox9, Col2, and Col1 in hNPCs co-cultured with hADSCs or MFAT were measured on days 7 and 14, and normalized to 18 s and to the control group. (B) Protein expression of aggrecan, SOX9, COL2, and COL1 in hNPCs co-cultured with hADSCs or MFAT were measured on day 21. (C-D) hNPCs co-cultured with hADSCs or MFAT by an indirect co-culture system were stained with alcian blue on day 21, and the area of blue staining was quantified. Data represent mean $\pm$ SEM; $N=9$; $**p < 0.01$. Scale bar $= 200$ μm.

of aggrecan, SOX9, and COL2 compared with those of all the groups. The ADSC group had higher expression of SOX9 than that of the control group, and no significant difference was observed between the ADSC and control groups regarding the expression levels of other proteins (Fig. 2B). Sulfate glycosaminoglycan (sGAG) synthesized by hNPCs was stained with alcian blue on day 21. The MFAT group showed deeper staining compared with that of the other two groups, indicating that the hNPCs co-cultured with MFAT synthesized more GAG than the other groups (Fig. 2C). We also quantified the area of alcian blue staining, and the results showed that the hNPCs co-cultured with MFAT had a higher percentage of area compared with that of the other groups ($p < 0.01$, Fig. 2D).

Effects of Co-culture on the Inflammation of hNPCs

We measured the expression levels of proinflammatory cytokine genes to show the effects of MFAT and hADSCs on the inflammation of hNPCs. hNPCs cultured without ADSCs or MFAT in acidic environments were used as the control group. The mRNA expression of TNF-α, IL-1β, and IL-6 was evaluated after 7 days of co-culture. The expression levels of TNF-α, IL-1β, and IL-6 in the ADSC group were almost 8.79, 6.49, and 14.46-fold higher, respectively, than those of the control group ($p < 0.01$). No significant difference was observed between the control and MFAT groups ($p > 0.05$, Fig. 3A–C).
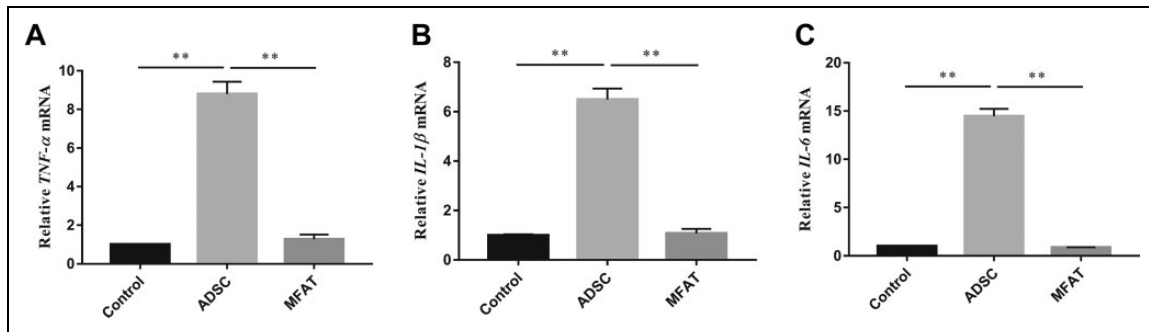
Figure 3. Effects of co-culture on the inflammation of hNPCs. Gene expressions of (A) TNF-α, (B) IL-1β, and (C) IL-6 in hNPCs co-cultured with hADSCs or MFAT were measured on day 7 and normalized to 18 s and to the control group. Data represent mean $\pm$ SEM; N=9; **p < 0.01.

Effects of hNPCs on the Differentiation of hADSCs and Cells in MFAT

The gene and protein expression levels of KRT19, PAX1, GPC3, and GDF10 were measured by PCR and western blotting. KRT19, PAX1, and GPC3 indicate NP-like differentiation of stem cells, while GDF10 is a specific marker of chondrogenic differentiation. After co-culture with hNPCs, cells in MFAT showed an increase in the gene expression of *Krt19*, *Pax1*, and *Gpc3* at each time point, especially on day 14 (p < 0.01). The gene and protein expression levels of GPC3 also increased after hADSCs were co-cultured with hNPCs on day 14 (p < 0.01). Both hADSCs and cells in MFAT showed an increase in the gene expression levels of *Gdf10* on day 7 after co-culture with hNPCs (p < 0.01). However, no significant difference was observed in the MFAT or MFAT+NPC groups on day 14 (p > 0.05), while the ADSC+NPC group had higher gene (p < 0.01) and protein expression of GDF10 than the ADSC group. The ADSC+NPC group also had higher gene (p < 0.05) and protein expression of GDF10 compared with those of the MFAT+NPC group (Fig. 4).

Radiographic and MRI Assessment of Discs in a Pig Disc Degeneration Model

As shown in Fig. 5A and B, the disc height of the degeneration and ADSCs groups was significantly lower than that of the control group after week 0 (p < 0.01). Although no significant difference was observed between the control and MFAT groups in images after week 4 (p > 0.05), the quantitative analysis of disc height showed that the DHI% in the MFAT group was lower than that of the control group at each time point (p < 0.01). The MFAT group (85.62 $\pm$ 2.00% and 83.52 $\pm$ 2.95%, respectively) had a higher DHI% than the degeneration (79.36 $\pm$ 1.15% and 74.86 $\pm$ 4.00%, respectively) and ADSCs (78.24 $\pm$ 2.00% and 75.12 $\pm$ 3.95%, respectively) groups after weeks 8 and 16 (p < 0.01). The MRI results

revealed the water content and structure of the NP. Compared with the MRI indexes of the degeneration (2162.92 $\pm$ 99.93, 1220.14 $\pm$ 16.95, and 1271.15 $\pm$ 125.71 mm^{2}GY, respectively) and ADSCs (2393.12 $\pm$ 246.24, 1251.70 $\pm$ 72.81, and 1410.59 $\pm$ 120.80 mm^{2}GY, respectively) groups, the MFAT group (3926.84 $\pm$ 268.71, 3565.00 $\pm$ 226.84, and 3928.20 $\pm$ 81.94 mm^{2}GY, respectively) had a higher MRI index on weeks 4, 8, and 16 (p < 0.01). The degeneration group had a lower MRI index than the other groups after week 4 (p < 0.01), while the control group had a higher MRI index than the other groups at each time point (p < 0.01, Fig. 5C and D).

Histological, Immunohistochemical and Biochemical Analysis of the NP

H&E staining of the IVDs showed that the NP in the control group was well organized with cells and ECM, while the degenerated NP had a destroyed structure and disorganized lamellar sheets of annulus fibrosus (AF). Injection of ADSCs did not repair the structure of NP after 16 weeks. The NP in the MFAT group had a regular distribution of ECM and cells, and the borders of NP and AF were distinguishable. S-O staining showed the deposition of proteoglycans in each group. The proteoglycans in the degeneration and ADSCs groups were significantly decreased compared with that of the control group. The MFAT group showed stronger staining than the degeneration group. The distribution of collagen II could be detected easily in the control and MFAT groups. However, few areas were immunopositive for collagen II in the degeneration and ADSCs groups (Fig. 6A). We also quantified the sGAG and collagen content by Blyscan and hydroxyproline assays. The MFAT group had higher sGAG content than those of the degeneration and ADSCs groups (p < 0.01), and no significant difference was observed in the sGAG content between the control and MFAT groups (p > 0.05, Fig. 6B). The hydroxyproline content of the control group was significantly higher than those of all the other
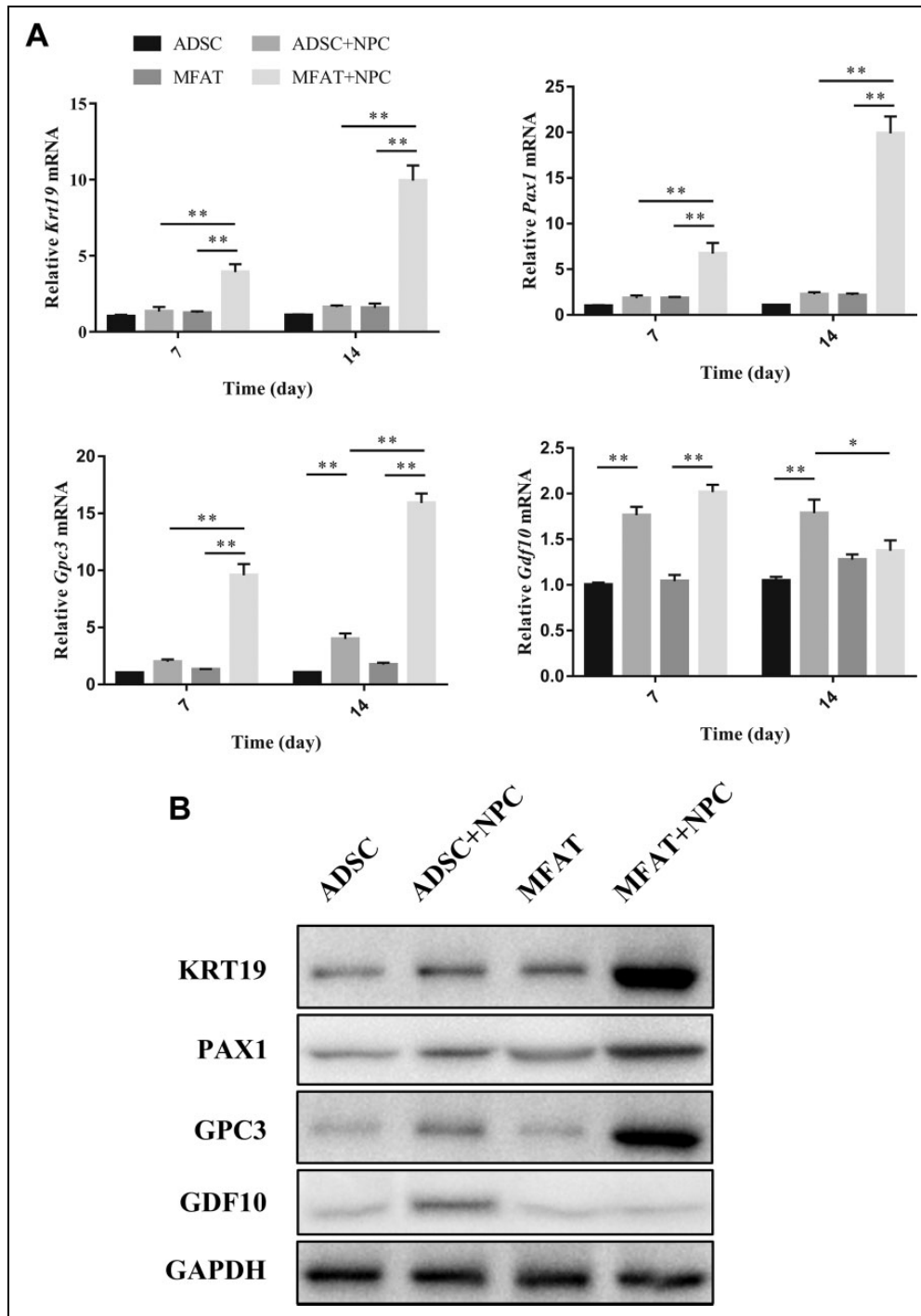
Figure 4. Effects of hNPCs on the differentiation of hADSCs and cells in the MFAT. (A) Gene expressions of Krt19, Pax1, Gpc3, and Gdf10 in each group were measured on days 7 and 14, and normalized to 18 s and to the control group. (B) Protein expression of KRT19, PAX1, GPC3, and GDF10 in each group was measured on day 14. Data represent mean ± SEM; $N=9$; *$p < 0.05$, **$p < 0.01$.

groups ($p < 0.01$). In addition, the MFAT group showed an increase in hydroxyproline content compared with the degeneration and ADSCs groups ($p < 0.01$, Fig. 6C). The histological, immunohistochemical, and biochemical analyses showed that MFAT could regenerate the degenerated NP to some extent, especially by increasing the ECM deposition.

Discussion

Stem cell transplantation has been widely used for the treatment of IVD degeneration[40,41]. However, isolation and *in vitro* amplification of stem cells prolong the preparation time and may alter the biology of the cells. Directly injecting
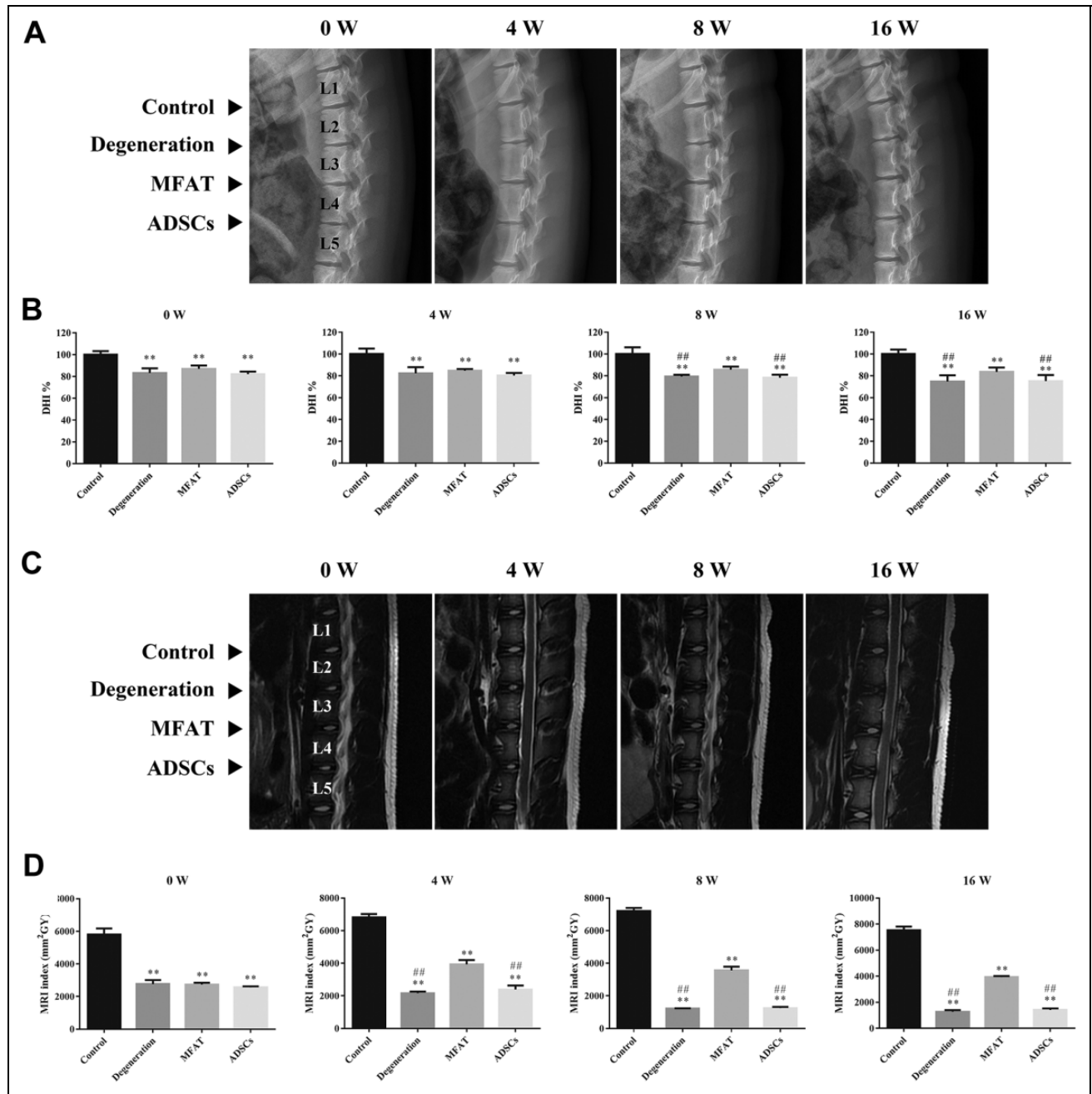
Figure 5. Radiographic and MRI assessment of discs in a pig disc degeneration model. (A) Representative radiographs of each group at 0, 4, 8, and 16 weeks after injection. The control, degeneration, MFAT, and ADSCs groups were detected. (B) DHI% was used to quantitatively represent the disc height changes. (C) Representative T2 MRI scans of the pig L1–L2, L2–L3, L3–L4, and L4–L5 lumber IVDs at 0, 4, 8, and 16 weeks after injection. (D) MRI index was used to quantitatively analyze the water content of the NP. Data represent mean $\pm$ SEM; $N=6$; $**p < 0.01$, vs. control group; $^{\#\#}p < 0.01$, vs. MFAT group.

adipose-derived SVF has healing potential in various degenerative conditions[42]. However, the direct use of the SVF showed negative effects in regenerating IVDs[29]. In this study, we used a mechanical method to isolate MFAT, which avoided the existence of collagenase in the injectable product. We first evaluated the effects of co-culture on matrix synthesis and inflammation of NPCs and the differentiation

of MFAT cells *in vitro*. We also investigated the regenerative effects of direct injection of MFAT in a pig disc degeneration model.

MFAT consists of a heterogeneous population of cells, ECM, and even fat. In this study, we regarded MFAT as an integral whole, and so fat or other components of MFAT contribute to the improvement in DHI%, MRI index, and
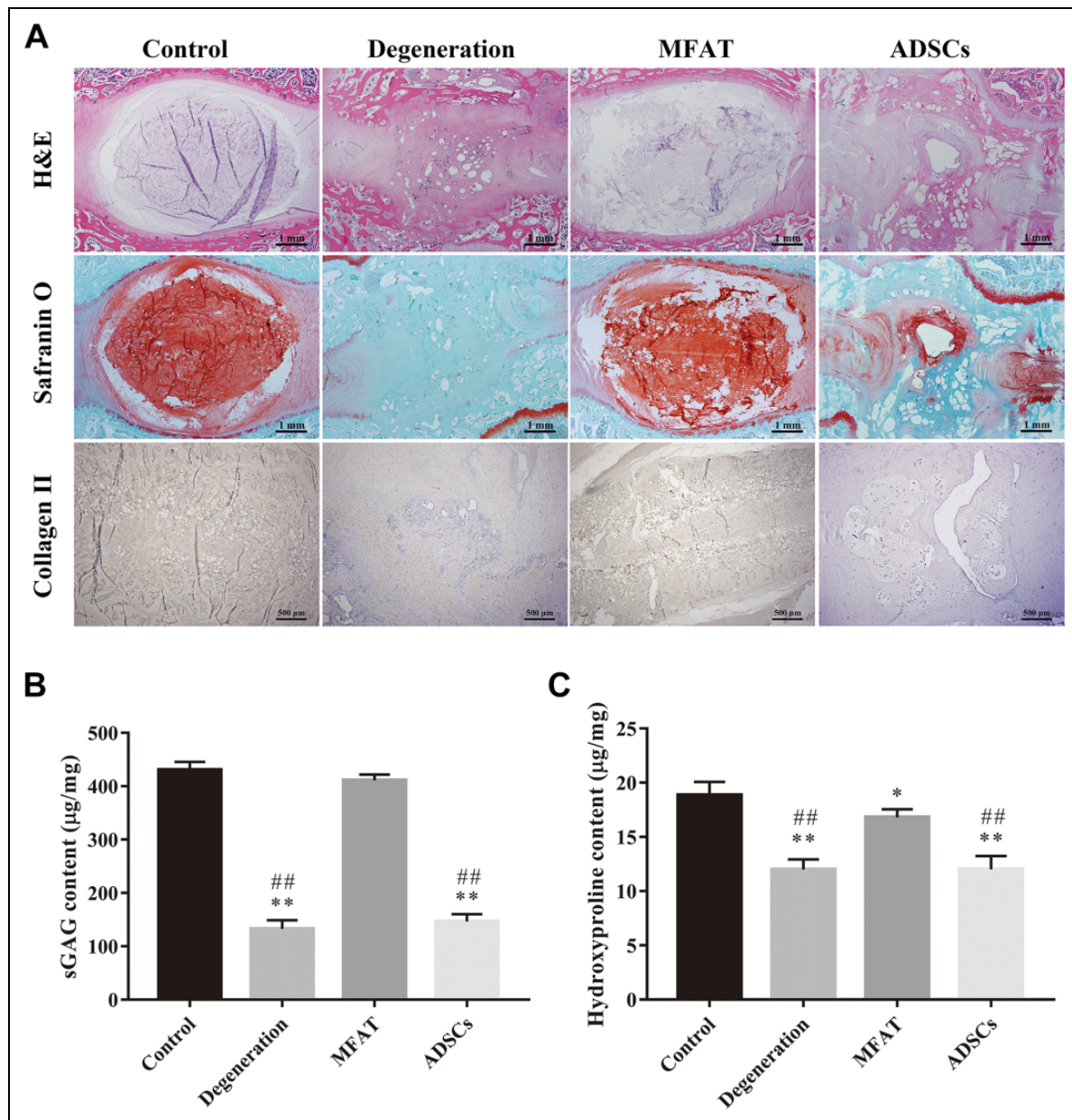
Figure 6. Histological, immunohistochemical, and biochemical analysis of the NP. Representative (A) H&E and Safranin O staining of disc samples from each group at 16 weeks after injection. Scale bar = 1 mm. Immunohistochemical detection of collagen II in the NP from the control, degeneration, MFAT, and ADSCs groups at 16 weeks after injection. Scale bar = 500 μm. The contents of (B) sGAG and (C) hydroxyproline in each group at 16 weeks after injection were quantified. Data represent mean ± SEM; N=6; *p < 0.05, **p < 0.01, vs. control group; ##p < 0.01, vs. MFAT group.

biochemical analysis, demonstrating the advantages of MFAT in regenerating the degenerative NP. The integral MFAT is superior to separated cells and fat because the ECM and fat in MFAT have the ability to fill space, and the cells in MFAT decrease inflammation and improve the matrix synthesis function of native NPCs. Our previous study demonstrated that simple space-filling material is not able to regenerate the degenerated NP and that simple cells do not survive well in the microenvironment of degenerative

NP[13]. Therefore, we think the regenerative effects in the degenerated NP depend on the integral MFAT. In addition, MFAT is advantageous because it is a minimally invasive injectable graft. ADSCs have been isolated from the adipose tissue and have shown promise in regenerative medicine[43]. However, recent studies have put adipose tissue on a par or even above ADSCs[44,45]. The heterogeneous cellular composition of MFAT may lead to better therapy outcomes in animal studies[46,47]. In the present study, we found that

during co-culture with MFAT, the matrix synthesis function of NPCs was significantly improved, whereas there was no change in the matrix synthesis function of NPCs when they were co-cultured with ADSCs. We think this is because the growth factors secreted by MFAT cells promote ECM synthesis in NPCs. MFAT cells secrete a variety of soluble growth factors such as FGF-2, vascular endothelial growth factor (VEGF), IGF-1 and platelet-derived growth factor (PDGF)-BB[42]. FGF-2 was reported to have the ability to maintain the differentiation potential and promote the ECM expression of NPCs[48]. VEGF plays a role in NPC survival and decreases apoptosis in NPCs[49]. IGF-1 and PDGF-BB stimulate the proliferation of NPCs by the activating the of extracellular-signal regulated kinase (ERK) and Akt signaling pathways[50].

We detected that ADSCs increased the expression of *TNF-α*, *IL-1β*, and *IL-6* in NPCs, which indicated that ADSCs alone increased the expression of proinflammatory molecules and promoted inflammation in NPCs. These results conflicted with previous studies. Shim et al. found that the proinflammatory cytokine genes *TNF-α*, *IL-1α*, *IL-1β*, and *IL-6* were significantly downregulated in NPCs after co-culturing with MSCs[33]. Cao et al. demonstrated that the inflammatory signaling molecule nuclear factor kappa B (NF-κB) was decreased after NPCs were co-cultured with MSCs[51]. In fact, the effects of MSCs on inflammation are complicated. Specific environmental factors are likely to affect the biological properties of ADSCs. A previous study demonstrated that ADSCs may exacerbate inflammation and induce apoptosis of HK-2 cells by increasing oxidative stress in the presence of cyclosporine[52]. In addition, MSCs intravenously injected into the lung microenvironment may also induce an inflammatory response by increasing TNF-α and IL-1β[53]. The acidic environment induced the production of proinflammatory cytokines, such as IL-1β and prostaglandin E2 (PGE$_2$), in ADSCs[54]. PGE$_2$ has a negative impact on IVD cell health and ECM homeostasis even after short-term exposure[55,56]. The culture medium used in this study had a pH of 6.8. Therefore, we hypothesize that the acidic environment in degenerative IVD may affect the function of ADSCs, and consequently, the proinflammatory cytokines secreted by ADSCs induced inflammation of NPCs. A previous study found that adipose tissues have the ability to reduce inflammatory factors such as *TNF-α* and *IL-6*[57]. Our study also demonstrated that MFAT did not cause inflammatory reactions even in an acidic environment.

The pig disc degeneration model was used in this study. Major advantages attributed to the porcine model include the similarity in size and shape of the discs to human IVDs[58,59]. A needle puncture model has been demonstrated to be feasible and widely used in previous studies[38,60]. The lumbar disc levels were not randomized because we hold the view that our results were independent of the implant locations. Pigs walk on four limbs and the mechanical load is almost evenly distributed on the lumbar discs. In addition, the ECM and cells in each lumbar disc are nearly the same. Our results

also showed that the DHI% and MRI index among the degeneration, MFAT, and ADSCs groups were similar and significantly lower than those of the control group at week 0. Sobajima et al. also considered that the degenerative progress of each lumbar disc is similar in a rabbit model[61]. Therefore, we think the results were not merely the effect of the implant location. In the present study, MFAT showed positive effects in regenerating the degenerated porcine NP. However, a severe inflammatory response was observed during regeneration with the SVF in a goat model[29]. We think the way adipose tissue is treated may be responsible for these differences. Collagenase was used to digest the SVF during isolation in the previous study, while a mechanical method was used to isolate MFAT in our study. MFAT isolated by mechanical methods has a high percentage of ADSCs, while the enzymatic treatment of cells affects the cell surface environment and glycocalyx compositions, which may influence cell adhesion and inflammatory responses[62,63]. The cells in the porcine NP may also be beneficial for the regenerative effects of MFAT because our *in vitro* study demonstrated that NPCs co-cultured with MFAT promoted the NP-like differentiation of MFAT cells.

There are still some limitations to our study. First, in addition to ADSCs, other cells in MFAT, such as dedifferentiated adipocytes, can also be differentiated into NP-like cells[64], and so we cannot identify which components in the SVF play roles in IVD regeneration. Second, we used an acidic environment to simulate the degenerative microenvironment, and other factors such as hypoxia exist in the degenerative IVD. We hypothesize that the real environment of degenerated IVDs may exacerbate inflammation and decrease ECM synthesis by MFAT and ADSCs[65]. Furthermore, notochordal cells are present during adult life in the porcine model, which may change the healing environment. In addition, the molecular mechanisms by which MFAT promotes ECM synthesis of NPCs *in vitro* require further study.

Conclusions

In this study, we isolated MFAT from subcutaneous adipose tissue by using a nonenzymatic method. MFAT has the ability to improve the matrix synthesis function of NPCs *in vitro*. MFAT does not cause inflammatory reactions in acidic environments when it is co-cultured with NPCs. In addition, NPCs also induce NP-like differentiation of MFAT cells. We further studied the regenerative effects of MFAT in a pig disc degeneration model. We demonstrated that MFAT can partly regenerate the degenerated NP after 16 weeks. Additional studies should be pursued to further understand the mechanisms of the NP regenerative effects of MFAT.

Statement of Human and Animal Rights

Statement of Informed Consent

Declaration of Conflicting Interests

Funding

ORCID iD

Xiaopeng Zhou https://orcid.org/0000-0002-0650-183X

Supplemental Material

Supplemental material for this article is available online.

References

1. Maniadakis N, Gray A. The economic burden of back pain in the UK. Pain. 2000;84(1):95–103.

2. Eyring EJ. The biochemistry and physiology of the intervertebral disk. Clin Orthop Relat Res. 1969;67:16–28.

3. Trout JJ, Buckwalter JA, Moore KC. Ultrastructure of the human intervertebral disc: II. cells of the nucleus pulposus. Anat Rec. 1982;204(4):307–314.

4. Chen J, Yan W, Setton LA. Molecular phenotypes of notochordal cells purified from immature nucleus pulposus. Eur Spine J. 2006;15(Suppl 3):S303–S311.

5. Lhonore A, Commere PH, Negroni E, Pallafacchina G, Friguet B, Drouin J, Buckingham M, Montarras D. The role of Pitx2 and Pitx3 in muscle stem cells gives new insights into P38alpha MAP kinase and redox regulation of muscle regeneration. Elife. 2018;7.

6. Du J, Zhen G, Chen H, Zhang S, Qing L, Yang X, Lee G, Mao HQ, Jia X. Optimal electrical stimulation boosts stem cell therapy in nerve regeneration. Biomaterials. 2018;181: 347–359.

7. Nair MB, Baranwal G, Vijayan P, Keyan KS, Jayakumar R. Composite hydrogel of chitosan-poly(hydroxybutyrate-co-valerate) with chondroitin sulfate nanoparticles for nucleus pulposus tissue engineering. Colloids Surf B Biointerfaces. 2015;136:84–92.

8. Zhu Y, Tan J, Zhu H, Lin G, Yin F, Wang L, Song K, Wang Y, Zhou G, Yi W. Development of kartogenin-conjugated chitosan-hyaluronic acid hydrogel for nucleus pulposus regeneration. Biomater Sci. 2017;5(4):784–791.

9. Tao Y, Zhou X, Liang C, Li H, Han B, Li F, Chen Q. TGF-beta3 and IGF-1 synergy ameliorates nucleus pulposus mesenchymal stem cell differentiation towards the nucleus pulposus cell type through MAPK/ERK signaling. Growth Factors. 2015;33(5–6):326–336.

10. Zhou X, Tao Y, Wang J, Liang C, Wang J, Li H, Chen Q. Roles of FGF-2 and TGF-beta/FGF-2 on differentiation of human mesenchymal stem cells towards nucleus pulposus-like phenotype. Growth Factors. 2015;33(1):23–30.

11. Stoyanov JV, Gantenbein-Ritter B, Bertolo A, Aebli N, Baur M, Alini M, Grad S. Role of hypoxia and growth and differentiation factor-5 on differentiation of human mesenchymal stem cells towards intervertebral nucleus pulposus-like cells. Eur Cell Mater. 2011;21:533–547.

12. Clarke LE, McConnell JC, Sherratt MJ, Derby B, Richardson SM, Hoyland JA. Growth differentiation factor 6 and transforming growth factor-beta differentially mediate mesenchymal stem cell differentiation, composition, and micromechanical properties of nucleus pulposus constructs. Arthritis Res Ther. 2014;16(2):R67.

13. Zhou X, Wang J, Fang W, Tao Y, Zhao T, Xia K, Liang C, Hua J, Li F, Chen Q. Genipin cross-linked type II collagen/chondroitin sulfate composite hydrogel-like cell delivery system induces differentiation of adipose-derived stem cells and regenerates degenerated nucleus pulposus. Acta Biomater. 2018;71:496–509.

14. Bertolo A, Mehr M, Aebli N, Baur M, Ferguson SJ, Stoyanov JV. Influence of different commercial scaffolds on the in vitro differentiation of human mesenchymal stem cells to nucleus pulposus-like cells. Eur Spine J. 2012;21(Suppl 6):S826–S838.

15. Gruber HE, Somayaji S, Riley F, Hoelscher GL, Norton HJ, Ingram J, Hanley EN, Jr. Human adipose-derived mesenchymal stem cells: serial passaging, doubling time and cell senescence. Biotech Histochem. 2012;87(4):303–311.

16. Izadpanah R, Kaushal D, Kriedt C, Tsien F, Patel B, Dufour J, Bunnell BA. Long-term in vitro expansion alters the biology of adult mesenchymal stem cells. Cancer Res. 2008;68(11): 4229–4238.

17. Zhang HT, Liu ZL, Yao XQ, Yang ZJ, Xu RX. Neural differentiation ability of mesenchymal stromal cells from bone marrow and adipose tissue: a comparative study. Cytotherapy. 2012;14(10):1203–1214.

18. Chen S, Deng X, Ma K, Zhao L, Huang D, Li Z, Shao Z. Icariin improves the viability and function of cryopreserved human nucleus pulposus-derived mesenchymal stem cells. Oxid Med Cell Longev. 2018;2018:3459612.

19. Tao Y, Zhou X, Liu D, Li H, Liang C, Li F, Chen Q. Proportion of collagen type II in the extracellular matrix promotes the differentiation of human adipose-derived mesenchymal stem cells into nucleus pulposus cells. Biofactors. 2016;42(2): 212–223.

20. Dicker A, Le Blanc K, Astrom G, van Harmelen V, Gotherstrom C, Blomqvist L, Arner P, Ryden M. Functional studies of mesenchymal stem cells derived from adult human adipose tissue. Exp Cell Res. 2005;308(2):283–290.

21. Gimble J, Guilak F. Adipose-derived adult stem cells: isolation, characterization, and differentiation potential. Cytotherapy. 2003;5(5):362–369.

22. Chae DS, Han S, Son M, Kim SW. Stromal vascular fraction shows robust wound healing through high chemotactic and epithelialization property. Cytotherapy. 2017;19(4):543–554.

23. Miranville A, Heeschen C, Sengenes C, Curat CA, Busse R, Bouloumie A. Improvement of postnatal neovascularization by human adipose tissue-derived stem cells. Circulation. 2004; 110(3):349–355.

24. Han J, Koh YJ, Moon HR, Ryoo HG, Cho CH, Kim I, Koh GY. Adipose tissue is an extramedullary reservoir for functional hematopoietic stem and progenitor cells. Blood. 2010;115(5): 957–964.

25. Usuelli FG, Grassi M, Maccario C, Vigano M, Lanfranchi L, Alfieri Montrasio U, de Girolamo L. Intratendinous adipose-derived stromal vascular fraction (SVF) injection provides a safe, efficacious treatment for Achilles tendinopathy: results of a randomized controlled clinical trial at a 6-month follow-up. Knee Surg Sports Traumatol Arthrosc. 2018;26(7):2000–2010.

26. Tissiani LA, Alonso N. A prospective and controlled clinical trial on stromal vascular fraction enriched fat grafts in secondary breast reconstruction. Stem Cells Int. 2016;2016:2636454.

27. Comella K, Silbert R, Parlo M. Effects of the intradiscal implantation of stromal vascular fraction plus platelet rich plasma in patients with degenerative disc disease. J Transl Med. 2017;15(1):12.

28. Nguyen A, Guo J, Banyard DA, Fadavi D, Toranto JD, Wirth GA, Paydar KZ, Evans GR, Widgerow AD. Stromal vascular fraction: a regenerative reality? part 1: Current concepts and review of the literature. J Plast Reconstr Aesthet Surg. 2016; 69(2):170–179.

29. Detiger SE, Helder MN, Smit TH, Hoogendoorn RJ. Adverse effects of stromal vascular fraction during regenerative treatment of the intervertebral disc: observations in a goat model. Eur Spine J. 2015;24(9):1992–2000.

30. Desando G, Bartolotti I, Martini L, Giavaresi G, Nicoli Aldini N, Fini M, Roffi A, Perdisa F, Filardo G, Kon E, Grigolo B. Regenerative features of adipose tissue for osteoarthritis treatment in a rabbit model: enzymatic digestion versus mechanical disruption. Int J Mol Sci. 2019;20(11):E2636.

31. Allon AA, Butcher K, Schneider RA, Lotz JC. Structured coculture of mesenchymal stem cells and disc cells enhances differentiation and proliferation. Cells Tissues Organs. 2012; 196(2):99–106.

32. Strassburg S, Richardson SM, Freemont AJ, Hoyland JA. Co-culture induces mesenchymal stem cell differentiation and modulation of the degenerate human nucleus pulposus cell phenotype. Regen Med. 2010;5(5):701–711.

33. Shim EK, Lee JS, Kim DE, Kim SK, Jung BJ, Choi EY, Kim CS. Autogenous mesenchymal stem cells from the vertebral body enhance intervertebral disc regeneration via paracrine interaction: an in vitro pilot study. Cell Transplant. 2016; 25(10):1819–1832.

34. Zuk PA, Zhu M, Mizuno H, Huang J, Futrell JW, Katz AJ, Benhaim P, Lorenz HP, Hedrick MH. Multilineage cells from human adipose tissue: implications for cell-based therapies. Tissue Eng. 2001;7(2):211–228.

35. Han B, Wang HC, Li H, Tao YQ, Liang CZ, Li FC, Chen G, Chen QX. Nucleus pulposus mesenchymal stem cells in acidic conditions mimicking degenerative intervertebral discs give better performance than adipose tissue-derived mesenchymal stem cells. Cells Tissues Organs. 2014;199(5–6):342–352.

36. Li H, Liang C, Tao Y, Zhou X, Li F, Chen G, Chen QX. Acidic pH conditions mimicking degenerative intervertebral discs impair the survival and biological behavior of human adipose-derived mesenchymal stem cells. Exp Biol Med (Maywood). 2012;237(7):845–852.

37. Zhou Z, Bez M, Tawackoli W, Giaconi J, Sheyn D, de Mel S, Maya MM, Pressman BD, Gazit Z, Pelled G, Gazit D, et al. Quantitative chemical exchange saturation transfer MRI of intervertebral disc in a porcine model. Magn Reson Med. 2016;76(6):1677–1683.

38. Revell PA, Damien E, Di Silvio L, Gurav N, Longinotti C, Ambrosio L. Tissue engineered intervertebral disc repair in the pig using injectable polymers. J Mater Sci Mater Med. 2007; 18(2):303–308.

39. Liang CZ, Li H, Tao YQ, Peng LH, Gao JQ, Wu JJ, Li FC, Hua JM, Chen QX. Dual release of dexamethasone and TGF-beta3 from polymeric microspheres for stem cell matrix accumulation in a rat disc degeneration model. Acta Biomater. 2013; 9(12):9423–9433.

40. Sivakamasundari V, Lufkin T.Stemming the degeneration: IVD stem cells and stem cell regenerative therapy for degenerative disc disease. Adv Stem Cells. 2013;2013. doi:10.5171/ 2013.724547.

41. Richardson SM, Kalamegam G, Pushparaj PN, Matta C, Memic A, Khademhosseini A, Mobasheri R, Poletti FL, Hoyland JA, Mobasheri A.Mesenchymal stem cells in regenerative medicine: focus on articular cartilage and intervertebral disc regeneration. Methods. 2016;99:69–80.

42. Bora P, Majumdar AS. Adipose tissue-derived stromal vascular fraction in regenerative medicine: a brief review on biology and translation. Stem Cell Res Ther. 2017;8(1):145.

43. Suzuki E, Fujita D, Takahashi M, Oba S, Nishimatsu H. Adipose tissue-derived stem cells as a therapeutic tool for cardiovascular disease. World J Cardiol. 2015;7(8):454–465.

44. Charles-de-Sa L, Gontijo-de-Amorim NF, Maeda Takiya C, Borojevic R, Benati D, Bernardi P, Sbarbati A, Rigotti G. Antiaging treatment of the facial skin by fat graft and adipose-derived stem cells. Plast Reconstr Surg. 2015;135(4): 999–1009.

45. You D, Jang MJ, Kim BH, Song G, Lee C, Suh N, Jeong IG, Ahn TY, Kim CS. Comparative study of autologous stromal vascular fraction and adipose-derived stem cells for erectile function recovery in a rat model of cavernous nerve injury. Stem Cells Transl Med. 2015;4(4):351–358.

46. Semon JA, Zhang X, Pandey AC, Alandete SM, Maness C, Zhang S, Scruggs BA, Strong AL, Sharkey SA, Beuttler MM, Gimble JM, et al. Administration of murine stromal vascular fraction ameliorates chronic experimental autoimmune encephalomyelitis. Stem Cells Transl Med. 2013;2(10): 789–796.

47. van Dijk A, Naaijkens BA, Jurgens WJ, Nalliah K, Sairras S, van der Pijl RJ, Vo K, Vonk AB, van Rossum AC, Paulus WJ, van Milligen FJ, et al. Reduction of infarct size by intravenous injection of uncultured adipose derived stromal cells in a rat model is dependent on the time point of application. Stem Cell Res. 2011;7(3):219–229.

48. Tsai TT, Guttapalli A, Oguz E, Chen LH, Vaccaro AR, Albert TJ, Shapiro IM, Risbud MV. Fibroblast growth factor-2 maintains the differentiation potential of nucleus pulposus cells in vitro: implications for cell-based transplantation therapy. Spine (Phila Pa 1976). 2007;32(5):495–502.

49. Fujita N, Imai J, Suzuki T, Yamada M, Ninomiya K, Miyamoto K, Iwasaki R, Morioka H, Matsumoto M, Chiba K, Watanabe S, et al. Vascular endothelial growth factor-A is a survival factor for nucleus pulposus cells in the intervertebral disc. Biochem Biophys Res Commun. 2008;372(2):367–372.

50. Pratsinis H, Kletsas D. PDGF, bFGF and IGF-I stimulate the proliferation of intervertebral disc cells in vitro via the activation of the ERK and Akt signaling pathways. Eur Spine J. 2007; 16(11):1858–1866.

51. Cao C, Zou J, Liu X, Shapiro A, Moral M, Luo Z, Shi Q, Liu J, Yang H, Ebraheim N. Bone marrow mesenchymal stem cells slow intervertebral disc degeneration through the NF-kappaB pathway. Spine J. 2015;15(3):530–538.

52. Chung BH, Lim SW, Doh KC, Piao SG, Heo SB, Yang CW. Human adipose tissue derived mesenchymal stem cells aggravate chronic cyclosporin nephrotoxicity by the induction of oxidative stress. PLoS One. 2013;8(3):e59693.

53. Hoogduijn MJ, Roemeling-van Rhijn M, Engela AU, Korevaar SS, Mensah FK, Franquesa M, de Bruin RW, Betjes MG, Weimar W, Baan CC. Mesenchymal stem cells induce an inflammatory response after intravenous infusion. Stem Cells Dev. 2013;22(21):2825–2835.

54. Borem R, Madeline A, Bowman M, Gill S, Tokish J, Mercuri J. Differential effector response of amnion- and adipose-derived mesenchymal stem cells to inflammation; implications for intradiscal therapy. J Orthop Res. 2019;37(11):2445–2456.

55. Vo NV, Sowa GA, Kang JD, Seidel C, Studer RK. Prostaglandin E2 and prostaglandin F2alpha differentially modulate matrix metabolism of human nucleus pulposus cells. J Orthop Res. 2010;28(10):1259–1266.

56. Hiyama A, Yokoyama K, Nukaga T, Sakai D, Mochida J. Response to tumor necrosis factor-alpha mediated inflammation involving activation of prostaglandin E2 and Wnt signaling in nucleus pulposus cells. J Orthop Res. 2015;33(12): 1756–1768.

57. Premaratne GU, Ma LP, Fujita M, Lin X, Bollano E, Fu M. Stromal vascular fraction transplantation as an alternative therapy for ischemic heart failure: anti-inflammatory role. J Cardiothorac Surg. 2011;6:43.

58. Tong W, Lu Z, Qin L, Mauck RL, Smith HE, Smith LJ, Malhotra NR, Heyworth MF, Caldera F, Enomoto-Iwamoto M, Zhang Y. Cell therapy for the degenerating intervertebral disc. Transl Res. 2017;181:49–58.

59. Daly C, Ghosh P, Jenkin G, Oehme D, Goldschlager T. A review of animal models of intervertebral disc degeneration: pathophysiology, regeneration, and translation to the clinic. Biomed Res Int. 2016;2016:5952165.

60. Omlor GW, Nerlich AG, Wilke HJ, Pfeiffer M, Lorenz H, Schaaf-Keim M, Bertram H, Richter W, Carstens C, Guehring T. A new porcine in vivo animal model of disc degeneration: response of anulus fibrosus cells, chondrocyte-like nucleus pulposus cells, and notochordal nucleus pulposus cells to partial nucleotomy. Spine (Phila Pa 1976). 2009;34(25): 2730–2739.

61. Sobajima S, Kompel JF, Kim JS, Wallach CJ, Robertson DD, Vogt MT, Kang JD, Gilbertson LG. A slowly progressive and reproducible animal model of intervertebral disc degeneration characterized by MRI, X-ray, and histology. Spine (Phila Pa 1976). 2005;30(1):15–24.

62. Carelli S, Messaggio F, Canazza A, Hebda DM, Caremoli F, Latorre E, Grimoldi MG, Colli M, Bulfamante G, Tremolada C, Di Giulio AM, et al. Characteristics and properties of mesenchymal stem cells derived from microfragmented adipose tissue. Cell Transplant. 2015;24(7):1233–1252.

63. Bianchi F, Maioli M, Leonardi E, Olivi E, Pasquinelli G, Valente S, Mendez AJ, Ricordi C, Raffaini M, Tremolada C, Ventura C. A new nonenzymatic method and device to obtain a fat tissue derivative highly enriched in pericyte-like elements by mild mechanical forces from human lipoaspirates. Cell Transplant. 2013;22(11):2063–2077.

64. Nakayama E, Matsumoto T, Kazama T, Kano K, Tokuhashi Y. Transplantation of dedifferentiation fat cells promotes intervertebral disc regeneration in a rat intervertebral disc degeneration model. Biochem Biophys Res Commun. 2017;493(2): 1004–1009.

65. Kwon WK, Moon HJ, Kwon TH, Park YK, Kim JH. The Role of hypoxia in angiogenesis and extracellular matrix regulation of intervertebral disc cells during inflammatory reactions. Neurosurgery. 2017;81(5):867–875.